XLVI CILAMCE
VITÓRIA - ES - BRAZIL - 2025
XLVI IBERO-LATIN AMERICAN CONGRESS ON COMPUTATIONAL METHODS IN ENGINEERING

Multi-Objective Optimization of Steel and Concrete Composite Cellular Beams

[1a]Pedro Henrique Avancini Guimarães, [1b]Maria Célia Loss Brandão, [1c]Marcos Antônio Campos Rodrigues, [1d]Élcio Cassimiro Alves

[1]*Dept. of Civil Engineering, Federal University of Espírito Santo*
Avenue Fernando Ferrari, 514, 29075-910, Vitória/ES, Brazil
[a]pedro.a.guimaraes@edu.ufes.br, [b]maria.l.brandao@edu.ufes.br, [c]marcos.a.rodrigues@ufes.br, [d]elcio.alves@ufes.br

Abstract. With the continuous advancement of civil construction in Brazil and worldwide, there is a growing demand for structural systems capable of spanning longer distances using elements that are both economically and environmentally sustainable. In this context, cellular beams emerge as a promising alternative, as their manufacturing process allows for an increase in section inertia without a proportional increase in structural mass. This study presents a multi-objective optimization approach for composite steel–concrete cellular beams. The objective functions include minimizing CO_2 emissions and the energy used in construction, as well as maximizing load-bearing capacity. The design constraints were derived from established recommendations in the literature, considering that current Brazilian standards lack specific technical provisions for the design of such beams. To address the optimization problem, the Multi-Objective Particle Swarm Optimization (MOPSO) algorithm was implemented. The resulting Pareto fronts will be compared with single-objective optimization outcomes reported in the literature. The expected outcomes include assessing the efficiency of the algorithm in finding optimal solutions, as well as achieving beam designs that are both economically and environmentally efficient while offering enhanced structural performance.

Keywords: Composite Tubular Truss, Multi-Objective Optimization, Multi-Objective Particle Swarm Optimization

1 Introduction

Since the Industrial Revolution, natural resource exploitation has increased dramatically, driving technological and economic growth. This has improved living standards through advances in infrastructure, healthcare, and housing. However, the development model has relied on excessive raw materials and energy use, ignoring ecological limits. The rapid expansion of factories and industrial cities, along with a capital-driven production logic and the growth of the construction industry, has caused severe environmental impacts like pollution and greenhouse gas emissions. The construction sector is a major contributor, responsible for significant resource extraction, waste, and emissions. According to the Global Status Report for Buildings and Construction 2024/2025 [1], it consumes 32% of global energy and accounts for 34% of CO_2 emissions, with cement and steel representing 18%. This highlights the urgent need to address construction's environmental impact and pursue sustainable industrial development. Within this framework, the use of composite steel structures emerges as an alternative by reducing the use of steel and concrete, two materials that generate the highest CO_2 emissions in the construction sector during their production processes.

The application of optimization techniques in steel–concrete composite systems has been widely explored over the past decades, as evidenced by the works of Tormen et al. [2] (composite steel and concrete beams with welded sections), Kravanja et al. [3] (composite floor structures consisting of reinforced

concrete slabs and steel beams), Arpini et al. [4] (composite floor systems with full-web beams), Erlacher et al. [5] (composite tubular trusses), and Almeida and Carneiro [6] (steel–concrete composite bridges and reinforced concrete bridges). Similarly, optimization studies on cellular composite steel–concrete beams can be found in the works of Ramos and Alves [7] [8], Silva et al. [9], and Alves et al. [10]. However, in those studies, the optimization process considered only a single objective function, either cost or CO_2 emissions.

Given this context, the present work aims to propose a multi-objective formulation for cellular steel–concrete composite beams, considering the minimization of CO_2 emissions and the energy consumption involved in their production process, and the maximization of the beam's load-bearing capacity. The design constraints are based on the provisions suggested by Lawson and Hicks [11]. The Multi-Objective Particle Swarm Optimization (MOPSO) method proposed by Coelho [12] will solve the problem and generate the Pareto fronts.

2 The Optimization Problem Formulation

In the multi-objective formulation for the design of composite steel and concrete tubular truss beams, the objectives of minimizing CO_2 emissions and energy consumption during the construction process, and maximizing the beam's load-carrying capacity, are considered as follows:

$$\begin{aligned} Min\ CO_2(kgCO_2) \\ = CO_{2,steel} + CO_{2,cut} + CO_{2,weld} + CO_{2,formwork} + CO_{2,concrete} \\ + CO_{2,connector} + CO_{2,mesh} \end{aligned} \tag{1}$$

$$\begin{aligned} Min\ EE(kW) = EE_{,steel} + EE_{,cut} + EE_{,weld} + EE_{,formwork} + EE_{,concrete} + EE_{,connector} \\ + EE_{,mesh} \end{aligned} \tag{2}$$

$$Max\ Load\ Bearing\ capacity = Q \tag{3}$$

In Equations (1) and (2), CO_2 e EE represent the CO_2 emissions and the energy expended for each component of the steel and concrete composite cellular beam, given respectively by the steel profile, cut, weld, steel deck formwork, studbolt connector, and the crack control mesh. Each term of the objective function is defined as follows:

$$[CO_2 \quad EE]_{steel} = \{A_{profile} - n_{opens}A_{opens}\}L_{beam}\rho_a\, S_{[CO_2 \quad EE]} \tag{4}$$

$$[CO_2 \quad EE]_{cut} = L_{cut}Cut_{[CO_2 \quad EE]} \tag{5}$$

$$[CO_2 \quad EE]_{weld} = L_{weld}W_{[CO_2 \quad EE]} \tag{6}$$

$$[CO_2 \quad EE]_{connector} = 2\ num_{connector}\ A_{cs}\ L_c\ \rho_a\ S_{[CO_2 \quad EE]} \tag{7}$$

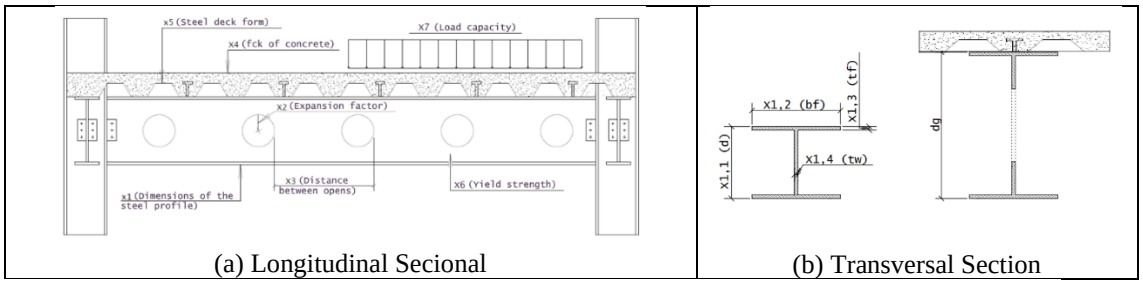
$$[CO_2 \quad EE]_{concrete} = Vol_{conc}\ C_{[CO_2 \quad EE]} \tag{8}$$

$$[CO_2 \quad EE]_{formwork} = Weight_{formwork}\ S_{[CO_2 \quad EE]} \tag{9}$$

$$[CO_2 \quad EE]_{rebars} = Weight_{rebars}\ Rebars_{[CO_2 \quad EE]} \tag{10}$$

In Equations (4) to (10), ρ_a represents the density of steel, considered as 7850 kg/m³; L_{beam} is the length of the beam; $S_{[CO_2 \quad EE]}$ corresponds to the CO_2 emissions and energy consumed per unit mass of steel produced; L_{cut} describes the shear length, which depends on the geometry of the openings; L_{weld} corresponds to the weld length, which also depends on the geometry of the openings; $Cut_{[CO_2 \quad EE]}$ represents the CO_2 emissions and energy consumed per unit length of the cellular beam during production; $W_{[CO_2 \quad EE]}$ corresponds to the CO_2 emissions and energy generated by the welding processes; A_{cs} describes the cross-sectional area of the connector; L_c corresponds to the length of the shear connector, given by the thickness of the concrete layer minus 10 mm; $C_{[CO_2 \quad EE]}$ describes the CO_2 emissions and energy consumed per unit volume of concrete during production; Vol_{conc} corresponds to the volume of concrete used in the slab; $Weight_{formwork}$ represents the weight of the final steel deck used in the solution; $Weight_{rebars}$ is the weight of the reinforcement used in the slab; $Rebars_{[co_2 \quad EE]}$ corresponds to the CO_2 emissions and energy associated with the reinforcement steel.

Figure 1 presents the design variables where the steel profile (x_1), the beam expansion factor (x_2), the spacing between openings (x_3), the slab's f_{ck} (x_4), the slab form (x_5), the steel grade for the profile (x_6), and the beam's load capacity (x_7). Table 1 presents the search space for the design variables.



(a) Longitudinal Secional (b) Transversal Section

Figure 1. Project Variables. Source: Adapted from Alves et *al*. [10].

Table 1. Design Variables Search Space

Design Variables	Search Space	Design Variables	Search Space
x_1	[1:1:88]	$x_5\ (m)$	[1.8:0.1:4]
x_2	[1.3:0.1:1.6]	$x_6\ (MPa)$	[345,415,450,450,485]
x_3		$x_7\ (kN/m^2)$	[1.5:0.1:20]
$x_4 (MPa)$	[20:5:50]		

Table 2 presents the unit values of CO2 emission and energy of each material from Negrin et al.'s [13] research.

Table 2. Unit CO_2 Emissions and Energy Consumption Values for Each Material

Material	Unit	CO_2 emissions ($kgCO_2$)	Source	Energy (kWh)	Source
20 MPa Concrete	m³	140.05	Santoro e Kripka [14]	433.97	Extrapolation
25 MPa Concrete	m³	149.26		468.39	Negrin et al. [13]
30 MPa Concrete	m³	157.65		502.79	
35 MPa Concrete	m³	171.64		537.22	
40 MPa Concrete	m³	182.14		571.61	Extrapolation
45 MPa Concrete	m³	194.70		606.03	
50 MPa Concrete	m³	225.78		640.43	
Steel deck	m²	2.638	World Steel Association [15]	8.70	Negrin et al. [13]
CA60 Steel mesh	kg	3.01	Negrin et al. [13]	10.39	
ASTM A572 Gr. 50 Steel	kg	2.04		4.98	
ASTM A572 Gr. 60 Steel	kg	2.07		5.05	
ASTM A572 Gr. 65 Steel	kg	2.09		5.10	
ASTM A913 Gr. 65 Steel	kg	2.10		5.13	
ASTM A913 Gr. 70 Steel	kg	2.13		5.20	
Cut	kg	20.09		48.98	
Weld	kg	0.03		0.07	

3 Numerical Results

Three models from Alves et al. (2025) [10] were analyzed to illustrate the application of the proposed formulation. In that study, composite cellular steel–concrete beams with different opening types were optimized using PSO and GWO, aiming solely to minimize CO_2 emissions. The considered loads were 1.5 kN/m² (live), 0.5 kN/m² (dead), a slab span of 2.5 m, and steel with a yield strength (fy) of 345 MPa.

Table 3 compares the results of Alves et al. (2025) with those obtained in this work, including: (i) PSO with f_y variable as 345, 415, 450, 485; (ii) MOPSO for the same load level, and (iii) the minimum load using MOPSO. For consistency, the steel emission factor used by Alves et al. (2025) [10] (1.116 $kgCO_2/kg$) was adjusted to the CO_2-equivalent adopted here, which yields higher values as it includes other greenhouse gases.

Table 3. Comparative Analysis

	Span (m)	**Alves et al. (2025) (PSO)**	**Authors (PSO f_y optimized)**	**Ratio (Authors/Alves et al. (2025)) (PSO)**	**MOPSO Load (1.5kN/m², f_y optimized)**	**Ratio Authors (MOPSO/PSO) CO_2**
CO_2 Emission ($kgCO_2$)	7,5	1014,63	927,86	0,91	932,32	1,00
	10,0	1598,70	1536,62	0,96	1558,89	1,01
	12,5	2421,30	2418,10	1,00	2418,10	1,00
Energy (kW)	7,5	-	2282,29	-	2293,83	1,01
	10,0	-	3783,04	-	3844,19	1,02
	12,5	-	5951,13	-	5951,14	1,00
Geometry	7,5	W 310 x 21.0	W 250 x 17.9	-	W 310 x 32.7	-
	10,0	W 360 x 32.9	W 360 x 32.9	-	W 360 x 32.9	-
	12,5	W 460 x 52.0	W 460 x 52.0	-	W 460 x 52.0	-

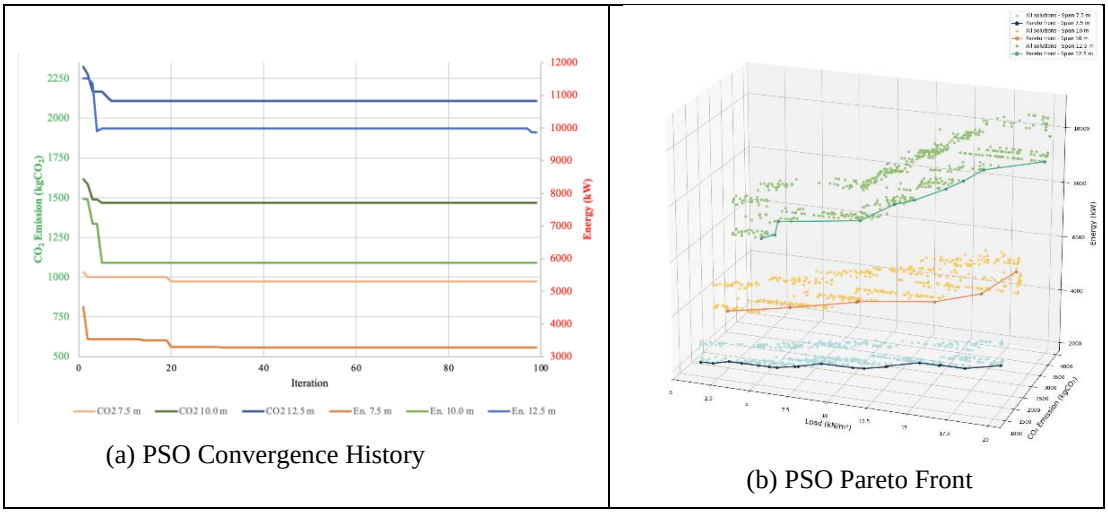
As shown in Table 3, when fy was considered a design variable, a reduction in CO2 emissions was observed compared to the results obtained by Alves et al. (2025) [10]. This reduction was approximately 4% for the 10.0 m span in the single-objective optimization with PSO, and it reached about 9% for the 7.5 m span. These results indicate that varying this parameter can yield significant gains in emission mitigation without compromising structural performance.

When comparing the solutions obtained through MOPSO for the same load level with those obtained via PSO, no significant differences in emission values were observed. The values are almost the same, demonstrating the precisionof the MOPSO method.

Regarding the energy results, it was observed that since the trend curve is parallel to that of emissions, the solutions obtained by MOPSO also presented values close to those of PSO with optimized fy . This behavior reinforces the efficiency of the multi-objective method in consistently obtaining good solutions when simultaneously aiming to minimize emissions and energy consumption.

In relation to the adopted profile geometries, it is noted that for the 10.0 and 12.5 m spans, the same profile was obtained in all analyses performed, which evidences the effectiveness of the implemented methodology. For the 7.5 m span, a profile reduction occurred when using PSO with optimized fy, suggesting that this method allowed for the exploration of more efficient alternatives as fy varied.

Figure 2 shows the convergence history of the PSO (a) and the Pareto fronts obtained via MOPSO (b) for the analyzed spans. This visualization allows for an understanding of the iterative process of solution improvement and the distribution of the solution triplets among the considered objectives.



(a) PSO Convergence History

(b) PSO Pareto Front

Figure 2. Convergence History and Pareto Fronts of the analyzed problems

As can be seen in Figure 2(a), the curves corresponding to CO_2 emissions and embodied energy exhibit parallel behavior throughout the iterations. This pattern indicates that there is no competing relationship between the two; in other words, the reduction of one tends to imply a proportional reduction of the other. Thus, the application of a multi-objective formulation considering only these two functions is not justified on its own. Therefore, a load maximization curve was introduced, which brings a new competing factor among the solutions, making it possible to more comprehensively explore the optimal solution space in a multi-objective analysis.

In Figure 2(b), the emission and energy values reached their maximum in the scenario with a 12.5 m span and a maximum load of 20 kN/m. This result highlights the influence of loading intensity on the simultaneous increase of emissions and energy consumption, reinforcing the importance of considering multiple objectives to avoid overdimensioned and environmentally less efficient solutions.

Table 4 – Final Geometries

Span(m)	PSO
7.5	Esquema de Corte Viga Interna W250x17.9 Perfil Aveolar Viga Interna ASTM A572 Gr. 50 401.6 mm 345.2505 mm 263.55 mm fy = 345 MPa
10	Esquema de Corte Viga Interna W360x32.9 Perfil Aveolar Viga Interna ASTM A572 Gr. 50 509.54 mm 403.82 mm 303.63 mm fy = 345 MPa
12.5	Esquema de Corte Viga Interna W460x52.0 Perfil Aveolar Viga Interna ASTM A572 Gr. 65 720 mm 617.76 mm 459 mm fy = 450 MPa

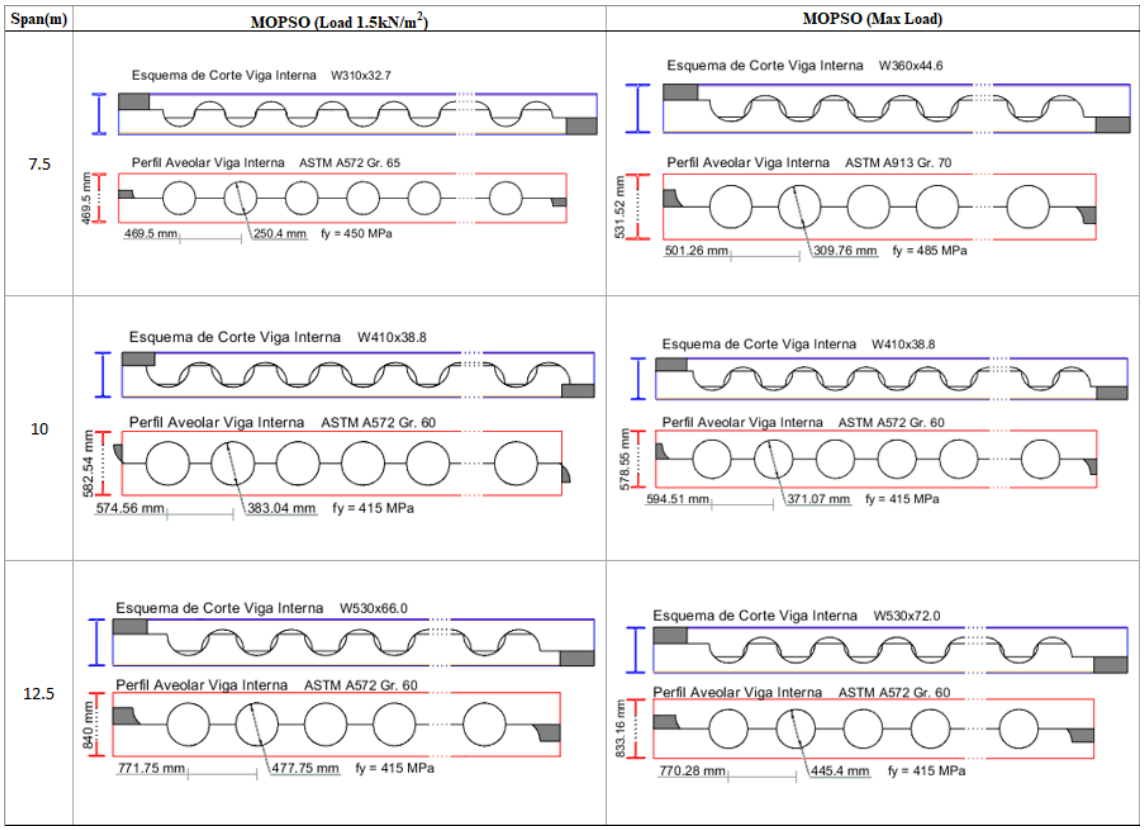


Table 4 presents the final geometries obtained for the cellular beams in each of the analyzed scenarios. This allows a direct comparison of the resulting structural configurations and highlights the differences in the selected sections according to variations in loads, spans, and the adopted optimization approach.

4 Concluding Remarks

The present work aimed to propose a multi-objective formulation for the design of steel-concrete composite cellular beams, simultaneously considering the minimization of CO_2 emissions and energy consumption in the production process and the maximization of the beam's load-bearing capacity.

Analyzing the results obtained for spans of 7.5, 10.0, and 12.5 meters, it was observed that the multi-objective formulation could identify a set of efficient solutions under multiple criteria. This highlights the significant impact that the choice of geometric and material parameters has on both structural performance and environmental indicators. It was also noted that it provided better solutions than those generated using PSO, demonstrating a greater capacity to converge towards more optimized alternatives.

The obtained Pareto fronts offer the best alternatives for each imposed loading, enabling a precise evaluation of how the proximity to one optimization objective affects the others. This visualization expands the possibility for informed decision-making, facilitating the selection of solutions that meet technical requirements without disregarding other criteria.

Thus, it is concluded that the proposed multi-objective formulation is an effective tool for designing steel-concrete composite cellular beams, offering a diverse set of optimized solutions that balance applied load, equivalent CO_2 emissions, and embodied energy. The results reinforce its potential for application and may serve as a basis for future studies considering additional variables, further broadening the relevance and applicability of the formulation.

Acknowledgements. The author would like to thank CAPES for supporting the postgraduate program in civil engineering at UFES and FAPES for the research grant provided to the fourth author.

Authorship statement. The author hereby confirms that they are the sole liable persons responsible for the authorship of this work and that all material that has been included herein as part of the present paper is either the property (and authorship) of the authors or has the permission of the owners to be included here.

References

[1] UNITED NATIONS ENVIRONMENT PROGRAMME. Global Status Report for Buildings and Construction 2024/25: Towards a zero-emissions, efficient and resilient buildings and construction sector. 2024. Disponível em: https://globalabc.org/resources/publications/2024-global-status-report-buildings-and-construction. Acesso em: 26 mai. 2025.

[2] TORMEN AF, PRAVIA ZMC, RAMIRES FB, KRIPKA M. (2020) Optimization of steel-concrete composite beams considering cost and environmental impact. Steel and Composite Structures, v.34, n°3, p.409-421. https://doi.org/10.12989/scs.2020.34.3.409, 2020.

[3] KRAVANJA, S.; KLANŠEK, U.; ŽULA, T. Mass, Direct Cost and Energy Life-Cycle Cost Optimization of Steel-Concrete Composite Floor Structures. Applied Sciences, [s. l.], v. 11, n. 21, 10316, p. 1-23, nov. 2021.

[4] ARPINI, P. A. T.; LOUREIRO, M. C.; BREDA, B. D.; CALENZANI, A. F.; ALVES, É. C. Optimum design of a composite floor system considering environmental and economic impacts. Revista IBRACON de Estruturas e Materiais, [s. l.], v. 15, n. 3, e15302, 2022.

[5] ERLACHER, G.; CALENZANI, A. F. G.; ALVES, É. C. Topological optimization of composite trusses considering CO2 emission via metaheuristics algorithms. Revista IBRACON de Estruturas e Materiais, [s. l.], v. 16, n. 6, e16606, 2023.

[6] ALMEIDA, D. C. B.; CARNEIRO, A. M. P. Environmental impact of steel/concrete composite bridges and reinforced concrete bridges: a comparative analysis through Life Cycle Assessment. Ambiente Construído, Porto Alegre, v. 25, e135202, p. 1-16, jan./dez. 2025.

[7] RAMOS, J. R. S.; ALVES, É. C. Análise numérica dos modos de colapso no dimensionamento otimizado de vigas mistas celulares. Revista da Estrutura de Aço, [s. l.], v. 9, n. 2, p. 222-240, ago. 2020.

[8] RAMOS, J. R. S.; ALVES, É. C. Numerical analysis of collapse modes in optimized design of alveolar Steel-concrete composite beams via genetic algorithms. Rem - International Engineering Journal, v. 74, p. 173-181, 2021.

[9] SILVA, G. F. ; KRIPKA, M. ; ALVES, E.C. . CO2 emission optimization of composite floor systems with cellular beams via metaheuristics algorithms. Structural Engineering And Mechanics, v. 89, p. 453-466, 2024.

[10] ALVES, É. C.; KRIPKA, M.; SILVA, G. F.; CALENZANI, A. F. G. Optimization of CO2 emissions of composite alveolar beams considering manufacturing constraints. REM, International Engineering Journal, Ouro Preto, v. 78, n. 2, e240041, p. 1-11, abr./jun. 2025.

[11] LAWSON, R. M.; HICKS, S. J. Design of Composite Beams with Large Web Openings: In accordance with Eurocodes and the UK National Annexes. Ascot, Berkshire: SCI, 2011.

[12] COELLO, C. A. C.; PULIDO, G. T.; LECHUGA, M. S. Handling multiple objectives with particle swarm optimization. IEEE Transactions on Evolutionary Computation, [s. l.], v. 8, n. 3, p. 256-279, jun. 2004.

[13] NEGRIN, I.; KRIPKA, M.; YEPES, V. Design optimization of a composite typology based on RC columns and THVS girders to reduce economic cost, emissions, and embodied energy of frame building onstruction. Energy and Buildings, [s. l.], v. 336, p. 115607, mar. 2025.

[14] SANTORO, J. F.; KRIPKA, M. Minimizing environmental impact from optimized sizing of reinforced concrete elements. Computers and Concrete, Daejeon, v.25, n. 2, p. 111-118, jan. 2020

[15] WORLD STEEL ASSOCIATION. Life Cycle Inventory (LCI) data for steel products. Brussels, Belgium: World Steel Association, 2021.